Phase of reflection high-energy electron-diffraction intensity oscillations during molecular-beam-epitaxy growth of GaAs(100)

J. Resh, K. D. Jamison, J. Strozier,* A. Bensaoula, and A. Ignatiev
Space Vacuum Epitaxy Center, University of Houston, Houston, Texas 77004
(Received 13 July 1989)

The intensities of several reflection high-energy electron-diffraction beams have been recorded simultaneously at varying angles of incidence and crystal substrate azimuth angles during molecular-beam-epitaxial growth of GaAs(100). Strong oscillations in the intensities of specular and nonspecular beams with same period but varying phases have been measured. The phase of the oscillations of the various beams has been found to vary with incident and azimuthal angle. A kinematic calculation based upon a simple model for epitaxial growth is presented, and its prediction concerning phase is compared with the experimental results. The results are also examined with regard to recent studies of the role of Kikuchi processes on the phase of the specular beam.

INTRODUCTION

One of the most notable and widely used aspects of reflection high-energy electron diffraction (RHEED) during molecular-beam-epitaxy (MBE) growth is the phenomenon of oscillations in the intensity of the specular beam in the diffraction pattern. It has been well established that the period of these oscillations corresponds exactly to the growth rate of 1 monolayer when epitaxy proceeds in a layer-by-layer nucleation and growth mode.[1] RHEED oscillations during MBE growth are thus routinely used for growth-rate determination and for calibration of the beam fluxes.

Intensity oscillations in nonspecular RHEED beams, while noted by other investigators,[2,3] have not been systematically studied, even though they sometimes have oscillations of greater amplitude than the specular beam. In this study, intensity oscillations in the 00 and 01 beams diffracted from the GaAs(100) surface have been systematically and simultaneously recorded as a function of incident angle and crystal azimuth during MBE growth. Although the oscillations from the various beams all have the same period, they exhibit a phase relationship with respect to one another that is very sensitive to the incident angle θ of the electron beam and the azimuthal angle φ of the substrate.

EXPERIMENTAL PROCEDURE

A video-camera-based intensity monitoring system has been developed at the University of Houston to simultaneously record RHEED intensities from multiple beams.[4] The monitoring system consists of a personal computer, a video digitizing board, a video monitor, and a video camera. To measure intensity oscillations, the video camera is focused on the RHEED screen of the MBE chamber, and the image is displayed on the video monitor. The user can create and manipulate the position of any number of "data windows," rectangular regions on the video monitor, of adjustable dimension. The intensity of the pixels enclosed by each data window is digitized by the video digitizing board and then integrated and stored in files for later analysis by associated software.

Sampling is done at a rate of 60 times a second for each window. The data is averaged in nonoverlapping groups of six points and then smoothed using a five-point rolling average to reduce noise, the principle source of which is the camera tube. The integrated intensity of the data windows, and therefore RHEED oscillations, can be displayed in real time on the computer monitor. The principle advantage of this system is its ability to monitor the intensity of up to ten diffracted beams simultaneously.

An undoped GaAs(100)$\pm$0.5° wafer cleaved into $\sim$1-cm squares was used as substrate material for GaAs homoepitaxial growth. After degreasing and etching, the GaAs was indium mounted into a three-inch molybdenum block. The molybdenum blocks were loaded into a Riber 32 MBE growth system, degassed, and transferred to the growth chamber. The oxide was removed by heating the substrates to 630 °C under an arsenic flux with the substrate continuously rotating. The sample was cooled to $\sim$600 °C and a 0.5-μm buffer layer of GaAs was grown. After growth, a sharp 2$\times$4 RHEED pattern was observed. To insure the best possible surface for additional layer growth measurement, the sample was then annealed in an arsenic flux at 600 °C for approximately 1 h.

All RHEED data was taken with the electron beam directed along the GaAs[110] direction with the twofold reconstruction visible on the RHEED screen. The incident angle was determined by measuring the distance between the specular beam and the straight-through beam on the RHEED screen. The incident angle θ was varied by moving the substrate in a direction normal to the surface and simultaneously adjusting the electron beam to keep it on the crystal surface. This arrangement to change the incident angle is awkward and, combined with the fact that the molybdenum holder blocks the straight-through beam at angles greater than 1.5°, is re-

sponsible for the significant error bars in the value of incident angle. Accurate determination of the azimuthal angle φ was achieved by measuring the difference in position of the 01 and $0\bar{1}$ beams.

Data windows of 1 pixel width bisecting the maximum intensity of the 01, 00, and $0\bar{1}$ beams were used, as shown in Fig. 1(b). During each data run, the intensities of all windows were recorded for a few seconds before growth while the substrate was in an arsenic flux. The Ga shutter was then opened for a period of roughly 60 sec and the RHEED oscillations were recorded during growth by the video system. Growth rates used were ~ 0.5 monolayers/sec. The substrate was annealed for at least 3 min between each growth run.

RESULTS

Figure 1(a) shows the RHEED oscillations for a typical growth run with oscillations in all three beams. While the period of oscillation is the same in all three beams, the phase is clearly different. Following the convention set by Zhang *et al.*,[5] the phase of a particular beam is determined by calculating the ratio $(t_{3/2}/T)$, where $t_{3/2}$ is the time from shutter opening to the second minimum of the oscillation, and T is the steady-state oscillation period (Fig. 1). A $(t_{3/2}/T)$ ratio of 1.5 indicates a "normal phase," i.e., the intensity begins at a maximum at zero layer coverage and falls to a minimum at half-layer coverage. A $(t_{3/2}/T)$ ratio of 1 or 2 corresponds to oscillations which begin at a minimum, i.e., 180° out of phase with the preceding description.

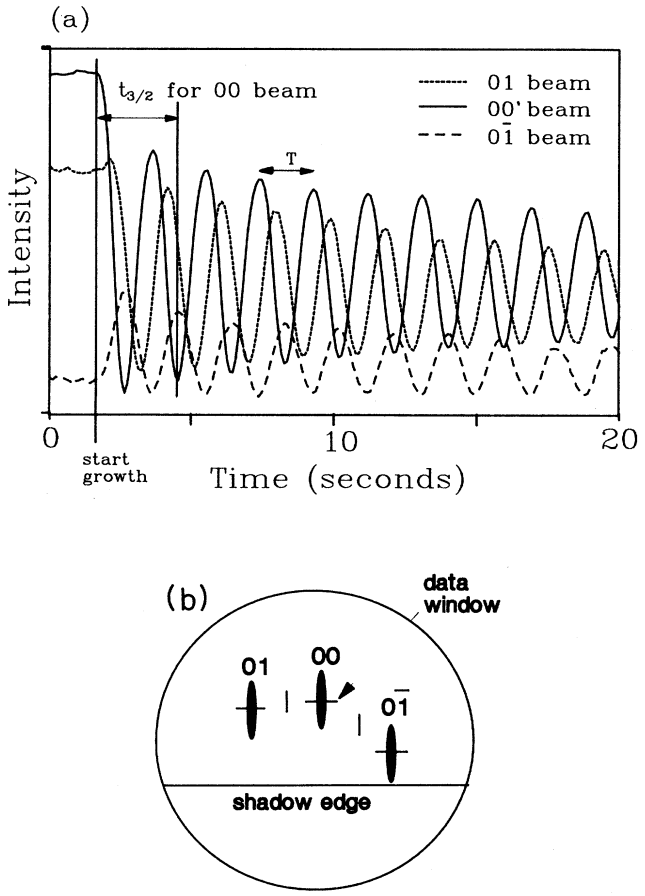

FIG. 1. (a) RHEED intensity oscillations for the 00, 01, and 01 beams. T is the period of oscillation. $t_{3/2}$ is the time from the start of growth to the second minimum of oscillation. (b) Schematic of image on RHEED screen, showing position of data windows.

Figure 2 is a plot of $(t_{3/2}/T)$ versus incident angle along the [110] direction for the 01, 00, and $0\bar{1}$ beams. Since this data was taken with the electron beam exactly aligned along a symmetry axis, the 01 and $0\bar{1}$ beams are in phase with one another and have identical $(t_{3/2}/T)$ ratios. The 01 and $0\bar{1}$ beams were not present for $\theta < 1.5°$, so that only the $(t_{3/2}/T)$ ratio for the 00 beam is plotted in this range. Also note that the $(t_{3/2}/T)$ ratio is confined to the range 1.0–2.0, in exactly the same way that an angular phase must lie between 0 and 360°. The curve for the 00 beam is thus not as discontinuous as it first appears. The peak in the angular range $\theta \sim 2.1$–$2.5°$, for example, is continuous with the data on either side of it, but must be drawn in a discontinuous fashion due to the definition of $(t_{3/2}/T)$. Note that the 00 and 01, $0\bar{1}$ beams are out of phase with each other except for the small incident angle range of 1.7–1.9°.

Figures 3(a) and 3(b) show plots of $t_{3/2}$ versus φ for two different incident angles. An azimuthal angle of 0.0° indicates exact alignment of the electron beam with the [110] direction. Due to the glancing angle of incidence, the 01 and $0\bar{1}$ beams are both present for only a very small azimuthal angular range. Note that the data is symmetric about a symmetry axis in the sample, $\varphi = 0°$, and that the 01 beam data is a mirror image of the $0\bar{1}$ beam data about $\varphi = 0°$. At the incident angle shown in Fig. 3(a), the 00 beam and the 01,$0\bar{1}$ beams were out of phase with each other at 0° azimuth. At the incident angle of $\theta = 1.9°$ shown in Fig. 3(b), the 00 and 01,$0\bar{1}$ beams begin in phase at $\varphi = 0°$ but rapidly go out of phase with each other. In both cases, the phase of the oscillations changes continuously and rapidly with changes in φ.

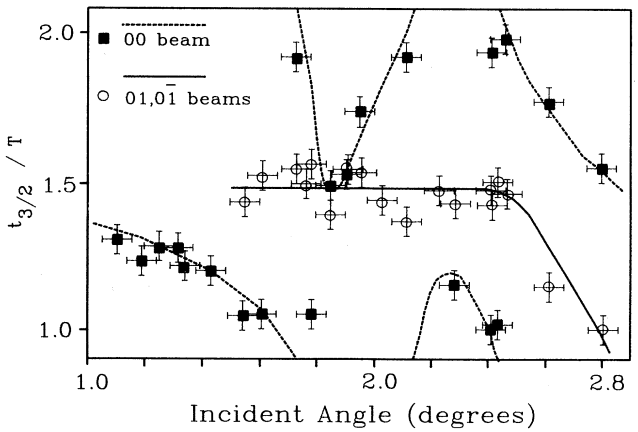

FIG. 2. $t_{3/2}/T$ ratio vs incident angle θ for the 00, 01, and the $0\bar{1}$ beams. The azimuthal angle $\varphi = 0°$. Lines were added to aid the eye only.

DISCUSSION

To better understand the oscillation phase results, a kinematic theory, analogous to calculations by Van Hove *et al.*,[6] and others,[7–9] is applied to a simple growth model. The model incorporates a simple cubic lattice crystal divided into domains of $N \times N$ lattice sites, as shown in Fig. 4. $P \times P$ lattice sites in each domain form an "island" at a higher level than the remaining sites. Growth occurs by successfully adding atoms to the $P \times P$ island, i.e., letting P approach N. The lattice is defined by $a\hat{\mathbf{i}}, b\hat{\mathbf{j}}, c\hat{\mathbf{k}}$, where a,b,c are the lattice constants in the x,y,z directions. K,L are indices that run from 1 to $K_{\max}$, and 1 to $L_{\max}$, respectively, and identify which domain the lattice site is in. m,n are indices that run from 1 to N and identify where in the domain the lattice site is located. l is an index that runs from 0 to infinity and identifies how many layers down from the surface the lattice site is located. Attenuation is incorporated using the column approximation and an attenuation constant α,[10] which is, as before, the ratio of the amplitude of the $(n+1)$ layer into the surface with the amplitude of the nth layer $(0<\alpha<1)$.

In the description of the electron scattering from the dominated sample, the usual kinematic sum of amplitudes is performed:

$$A = F(\theta,E) \sum_{\substack{\text{all} \\ \text{lattice} \\ \text{sites} \\ \mathbf{r}_j}} e^{i(\mathbf{S}\cdot\mathbf{r}_j)} \tag{1}$$

where $\mathbf{S}(=\mathbf{k}_f-\mathbf{k}_1)$ is the momentum transfer to the crystal and $F(\theta,E)$ is the atomic scattering factor. The amplitude is extended over the three regions in each domain: (i) all lattice sites in the $P \times P$ islands, (ii) all lattice sites in the rectangular region immediately above (i), and (iii) all lattice sites in the rectangular region to the right of (i) and (ii):

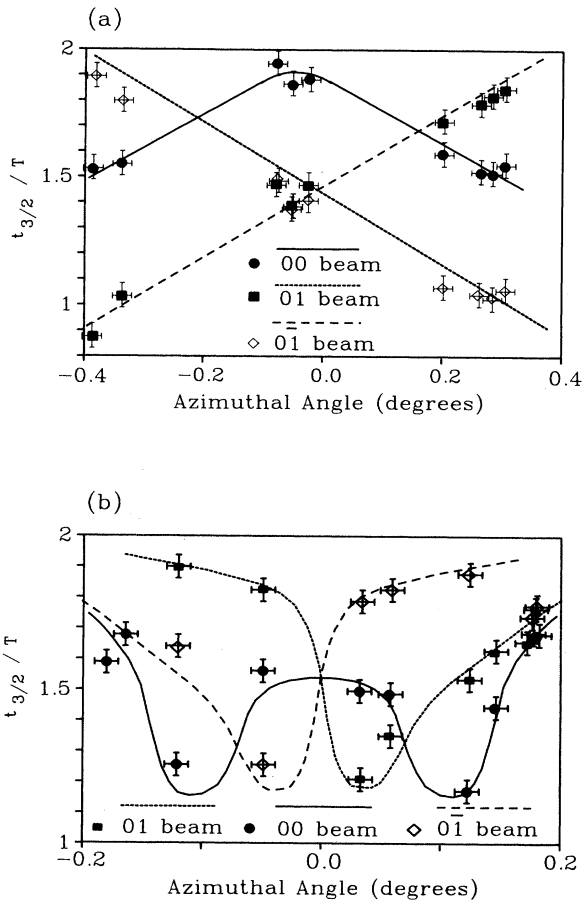

FIG. 3. (a) $t_{3/2}/T$ ratio vs azimuthal angle φ for the 00, 01, and $0\bar{1}$ beams. $\theta=2.1°$. (b) $t_{3/2}/T$ ratio vs azimuthal angle φ for the 00, 01, and $0\bar{1}$ beams. $\theta=1.9°$. Lines were added to aid the eye only.

$$\begin{aligned}\frac{A}{F(\theta,E)} = &\sum_{K=0}^{K_{\max}}\sum_{L=0}^{L_{\max}}\sum_{m=0}^{P}\sum_{n=0}^{P}\sum_{l=-1}^{\infty} e^{iS_x aNK} e^{iS_y bNL} e^{iS_x am} e^{iS_y bn} e^{-iS_z cl} \alpha^{l+1} \\ &+ \sum_{K=0}^{K_{\max}}\sum_{L=0}^{L_{\max}}\sum_{m=0}^{N-P}\sum_{n=0}^{N}\sum_{l=0}^{\infty} e^{iS_x aNK} e^{iS_y bNL} e^{iS_x aP} e^{iS_x am} e^{iS_y bn} e^{-iS_z cl} \alpha^{l} \\ &+ \sum_{K=0}^{K_{\max}}\sum_{L=0}^{L_{\max}}\sum_{m=0}^{P}\sum_{n=0}^{N-P}\sum_{l=0}^{\infty} e^{iS_x aNK} e^{iS_y bNL} e^{iS_x am} e^{iS_y bP} e^{iS_y bn} e^{-iS_z cl} \alpha^{l} .\end{aligned} \tag{2}$$

Simplification results in

$$\begin{aligned}\frac{A}{F(\theta,E)} = &\left[\frac{1-e^{iS_x aN(K_{\max}+1)}}{1-e^{iS_x aN}} \frac{1-e^{iS_y bN(L_{\max}+1)}}{1-e^{iS_y bN}} \frac{1}{1-a^{-iS_z cl}}\right] \\ &\times \left[\sum_{m=0}^{P} e^{iS_x am} \sum_{n=0}^{N-P} (e^{iS_y bn} e^{iS_y bp}) + \sum_{m=0}^{N-P} e^{iS_x am} \sum_{n=0}^{N} e^{iS_y bn} (e^{iS_y aP}) \alpha \sum_{m=0}^{P} e^{iS_x am} \sum_{n=0}^{P} e^{iS_y bn} \right. \\ &\left. + (-\alpha e^{iS_z c}) e^{iS_z c} \sum_{m=0}^{P} e^{iS_x am} \sum_{n=0}^{P} e^{iS_y bn}\right] .\end{aligned} \tag{3}$$

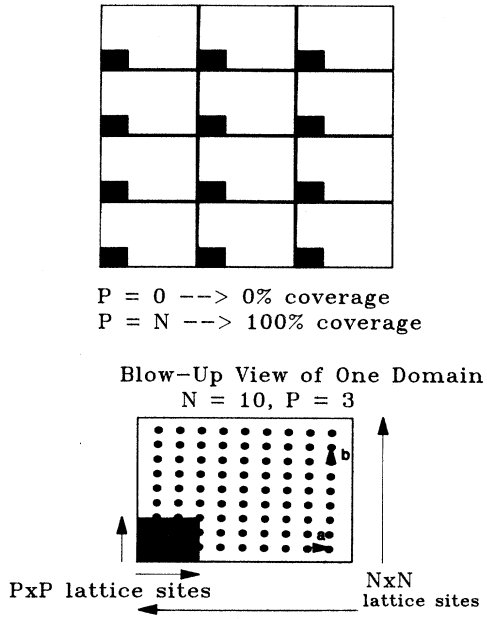

FIG. 4. Growth model, consisting of islands of dimension $P \times P$ lattice sites within domains of $N \times N$ lattice sites. Growth of a layer occurs as P goes from 0 to N.

Note that the result is independent of the areal distribution of the lattice sites in the $P \times P$ islands, suggesting more generality than the rather restricted growth model assumed.

The first term is the usual two-dimensional scattering expression from a semi-infinite crystal with attenuation. The second term takes a simplified form when the intensity of a diffracted beam is examined, i.e., when the Laue conditions are met. For a diffracted beam, $S_x a$ and $S_y b$ are reciprocal-lattice vectors. After substitution, the term in braces reduces to:

$$P^2(e^{iS_z c}-1)+N^2=N^2[R(e^{iS_z c}-1)+1]\,, \tag{4}$$

where $R\,(=P^2/N^2)$ is the surface coverage.

If $S_z c=2m\pi$, with m an integer, i.e., the "on-Bragg" condition, then $A \propto N^2$, and $I=AA^*=$constant. Therefore, there are no oscillations in any diffracted beam intensity for this condition of diffraction.

If $S_z c=(2m+1)\pi$, i.e., the "off-Bragg" condition, then $A \propto N^2(1-2R)$ and $I \propto N^4(1-2R)^2$, and oscillations are observed for all diffracted beams.

This last result predicts oscillations with a parabolic shape. The interesting feature is that the intensity minimum always occurs at half-layer coverage, $R=\frac{1}{2}$, with the intensity always dropping at the onset of growth. Thus, kinematic theory, in the column approximation with attenuation, predicts RHEED intensity oscillations in all of the diffracted beams when an "off-Bragg" condition is realized but with no phase shifts. Figures 2 and 3 clearly show, however, that significant phase differences between oscillations in different diffracted beams occur and are sensitive to the experimental geometry.

As simple kinematic theory does not predict phase differences between diffracted beams, a number of possibilities were investigated to understand these phase differences. First, an investigation was made as to whether the position of the data window on the diffraction streak (beam) had any effect on the phase of the beam. Data windows positioned at various places along the streak showed no changes in phase.

Next, the possible role of inelastic processes was examined. Recent works by Zhang *et al.*[5] and Crook *et al.*[11] suggest that interaction with Kikuchi lines may be responsible for the change of phase away from the expected $t_{3/2}/T=1.5$ for the specular beam. Kikuchi lines are caused by inelastic electrons elastically scattering off a lattice plane.[12] The number of inelastic electrons available for Kikuchi processes should be largest when the surface is in the highest degree of disorder. Kikuchi line intensity should therefore oscillate 180° out of phase with the "normal phase" of elastically scattered beams. In their paper, Crook *et al.* show several cases in which a Kikuchi line crosses near the specular beam and oscillates with a different phase than the elastically scattered peak of the specular beam. They concluded that interference between these Kikuchi line crossings and the specular beam results in a phase shifting of the oscillation observed at the specular position.

The data presented here, however, shows phase shifts in the 00, 01, and $0\bar{1}$ beams over a continuous range of incident and azimuthal angle, regardless of whether or not there are Kikuchi lines near the particular beam(s). Figure 5, for example, shows a growth run in which a Kikuchi line crossed the $0\bar{1}$ beam, but was far from the 00 and 01 beams. The phase difference between the 00 beam and the 01 beam for that run is, however, approximately equal in magnitude to the phase difference between the 00 beam and the $0\bar{1}$ beam, behavior similar to that when no

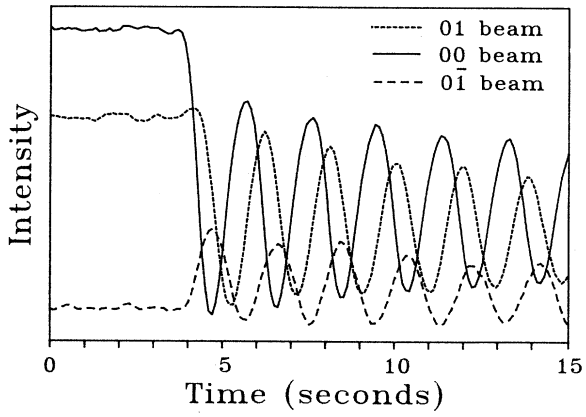

FIG. 5. RHEED oscillations in which a visible Kikuchi line crossed the 01 beam but did not cross the 00 or $0\bar{1}$ beams.

Kikuchi line crossings are noted. Furthermore, these phase shifts change continuously with azimuth, as shown in Fig. 3(a).

CONCLUSION

Significant phase differences have been observed between the RHEED intensity oscillations simultaneously measured for different diffracted beams. This observation cannot be explained by simple kinematic theory, which shows all beams oscillating with identical phase. Furthermore, these phase differences occur throughout incident angle-azimuthal angle parameter space and change in a continuous manner, regardless of the presence or absence of Kikuchi line crossings in the beams. It is, therefore, doubtful that the phase differences observed between different diffracted beams are caused by inelastic processes. Whether an elastic, multiple-scattering, dynamical approach can explain these phase differences needs to be determined. It is clear, however, that diffraction conditions (as opposed to growth conditions) can drastically affect the RHEED oscillation phase. As a result, it should be realized that the maximum intensity of a diffracted beam does not necessarily correspond to a completed layer during growth.

ACKNOWLEDGMENTS

Partial support for this work has been supplied by NASA under Grant No. NAGW-977 and the R. A. Welch Foundation. We would like to thank Richard Lyders-Gustafson for his invaluable assistance in the data analysis and associated required software.

---

*Permanent address: Empire College, State University of New York, Stony Brook, New York 11790.

[1]J. M. Van Hove, P. R. Pukite, and P. I. Cohen, J. Vac. Sci. Technol. B **1**, 741 (1983).

[2]J. H. Neave and B. A. Joyce, Appl. Phys. A **31**, 1 (1983).

[3]P. J. Dobson, B. A. Joyce, J. H. Neave, and J. Zhang, J. Cryst. Growth **81**, 1 (1987).

[4]J. S. Resh, J. Strozier, K. D. Jamison, and A. Ignatiev, Rev. Sci. Instrum. (to be published).

[5]J. Zhang, J. H. Neave, P. J. Dobson, and B. A. Joyce, Appl. Phys. A **42**, 317 (1987).

[6]J. M. Van Hove, P. R. Pukite, and P. I. Cohen, J. Vac. Sci. Technol. B **3**, 563 (1985).

[7]J. H. Neave, B. A. Joyce, P. J. Dobson, and N. Norton, Appl. Phys. A **31**, 1 (1983).

[8]A. Madhukar, S. V. Ghaisas, T. C. Lee, M. Y. Chen, P. Chen, J. Y. Kim, and P. G. Newmann, Proc. SPIE **524**, 78 (1985).

[9]B. F. Lewis, F. J. Grunthaner, A. Madhukar, T. C. Lee, and R. Fernandez, J. Vac. Sci. Technol. B **3**, 1317 (1985).

[10]M. B. Webb and M. G. Lagally, *Elastic Scattering of Low-Energy Electrons from Surfaces* (University of Wisconsin, Madison, Wisconsin, 1976), p. 301.

[11]G. E. Crook, E. G. Eyink, A. C. Campbell, D. R. Hinson, and B. G. Streetman, J. Vac. Sci. Technol. A (to be published).

[12]P. B. Hirsch, A. Howie, R. B. Nicholson, D. W. Pashley, and M. J. Whelen, in *Electron Microscopy of Thin Crystals* (Butterworths, Washington, 1965), p. 119.